Long vs short-term synaptic learning rules after optogenetic spike-timing-dependent plasticity

Margarita Anisimova, Bas van Bommel, Marina Mikhaylova, J. Simon Wiegert, Thomas G. Oertner†, Christine E. Gee†*

Center for Molecular Neurobiology Hamburg, University Medical Center Hamburg-Eppendorf, Hamburg, Germany.

† These authors contributed equally to this work

* Corresponding author: Christine E. Gee

Email: christine.gee@zmnh.uni-hamburg.de

ORCIDs: M. Anisimova 0000-0003-1557-7358, Bas van Bommel 0000-0003-2875-0447, J. Simon Wiegert 0000-0003-0893-9349, Marina Mikhaylova 0000-0001-7646-1346, Thomas G Oertner 0000-0002-2312-7528, Christine E Gee 0000-0003-0345-3665

Keywords: Synaptic plasticity, hippocampus, optogenetics, LTP, LTD.

Subject Area: Neuroscience

Author Contributions: Conceptualization, CEG, TGO, JSW; **Investigation,** MA, BvB, CEG; **Writing – Original Draft,** CEG, TGO, MA; **Writing – Review and Editing,** CEG, TGO, MA, BvB, JSW, MM; **Technical expertise,** TGO, CEG, MM; **Visualization,** MA, CEG, TGO; **Supervision,** CEG, TGO; **Project Funding Acquisition,** CEG, JSW. All authors approved the author list and final version.

This file includes:

Main Text
Figures 1 to 4
Supplementary Figures S1 to S6

Abstract

Spike-timing-dependent plasticity (STDP) is a candidate mechanism for information storage in the brain. However, it has been practically impossible to assess the long-term consequences of STDP because recordings from postsynaptic neurons last at most one hour. Here we introduce an optogenetic method to, with millisecond precision, independently control action potentials in two neuronal populations with light. We apply this method to study spike-timing-dependent plasticity (oSTDP) in the hippocampus and reproduce previous findings that depression or potentiation depend on the sequence of pre- and postsynaptic spiking. However, 3 days after induction, oSTDP results in potentiation regardless of the exact temporal sequence, frequency or number of pairings. Blocking activity between induction and readout prevented the synaptic potentiation, indicating that strengthened synapses have to be used to get strong. Our findings indicate that STDP potentiates synapses and that the change in synaptic strength persist to behaviorally relevant timescales.

Introduction

Attractive models of how memories form are based on observations that the strength of synapses change after coincident activity in the pre- and postsynaptic neurons, a process commonly referred to as spike-timing-dependent plasticity (STDP) (Gerstner *et al.*, 1996; Song, Miller and Abbott, 2000; van Rossum, Bi and Turrigiano, 2000; Masquelier, Guyonneau and Thorpe, 2009; Costa *et al.*, 2015). Indeed, STDP learning rules are now widely used for unsupervised learning and have been implemented to run on neuromorphic hardware (see e.g. 5–7). Timing-dependent long-term potentiation (tLTP) occurs when excitatory synaptic responses repeatedly precede postsynaptic action potentials, i.e. causal or Hebbian pairing. In contrast, timing-dependent long-term depression (tLTD) occurs when synaptic responses follow the postsynaptic action potentials, i.e. anti-causal pairing (Markram *et al.*, 1997; Bi and Poo, 1998; Debanne, Gähwiler and Thompson, 1998). However, STDP experiments are usually limited to 20-60 minutes, a period clearly not relevant for most forms of memory. This time limitation arises from the invasive nature of intracellular recordings, which are necessary to control postsynaptic spiking. In contrast, studies of synaptic plasticity using extracellular recordings to stimulate presynaptic axons and record ensemble responses from postsynaptic neurons can last several hours and even weeks when performed in vivo (Bliss and Lomo, 1973). Such studies have reported major differences in the mechanisms underlying early (~1-3 hours) and late (> 3 hours) LTP following short periods of intense presynaptic stimulation. For example, early hippocampal CA3-CA1 LTP depends on NMDA receptor activation, calcium-calmodulin dependent kinase II and the phosphorylation and postsynaptic insertion of AMPA receptors whereas late LTP also requires cAMP signaling and synthesis of new proteins (Malenka *et al.*, 1989; Frey, Huang and Kandel, 1993; Barria *et al.*, 1997; Hayashi *et al.*, 2000). LTD at CA3-CA1 synapses can also be long-lasting (Doyère *et al.*, 1996). LTD also depends on NMDA and/or metabotropic glutamate receptors and curiously, LTD induction can actually promote the subsequent induction of LTP (Parvez, Ramachandran and Frey, 2010). A recent study has successfully used extracellular paired stimulation of CA3 Schaffer collaterals and CA1 axons in the alveus in hippocampal slices to induce STDP thereby extending the observation window to 4 hours (Pang *et al.*, 2019). Our goal was to further extend the observation window to a time scale relevant for behavioral studies of memory.

Channelrhodopsins are ion channels that open in response to light, and since the discovery of channelrhodopsin-2 (Nagel *et al.*, 2003) have been widely used to stimulate neurons with light *in*

vitro and *in vivo* (e.g. Boyden *et al.*, 2005; Adamantidis *et al.*, 2007; Huber *et al.*, 2008). In recent years, many channelrhodopsin variants have been discovered or engineered with varying kinetics and spectral sensitivity (Hochbaum *et al.*, 2014; e.g. Klapoetke *et al.*, 2014). We reasoned that using opsins sensitive to different wavelengths of light, we could circumvent the need for intracellular/patch-clamp recordings and optically induce 'no-patch' STDP. Here, we present a two-color method to stimulate precisely timed action potentials in defined subsets of CA3 and CA1 pyramidal neurons for optogenetic induction of STDP (oSTDP). Whereas oSTDP induced classical tLTP and tLTD in short-term patch-clamp experiments, the outcome after 3 days was strong tLTP regardless of the activation sequence. Our findings support the conclusion that the short and long-term consequences of STDP are different.

Results

Independently spiking neurons using ChrimsonR and CheRiff

To achieve our goal of independently spiking pre- and postsynaptic neurons, we used the red light sensitive ChrimsonR (Klapoetke *et al.*, 2014) and the blue/violet light-sensitive CheRiff (Hochbaum *et al.*, 2014). ChrimsonR-tdTomato was expressed in a small subset of CA3 pyramidal neurons by local virus injection and several CA1 neurons were electroporated with DNA encoding CheRiff-eGFP (Fig. 1A). In order to visualize CheRiff-expressing CA1 neurons (hereafter referred to as CheRiff-CA1 neurons) without activating them we also included DNA encoding mKate2 in the electroporation mix. We waited 7-10 days for expression of both channelrhodopsins before starting the experiments.

Given that the threshold for light-induced APs is not only opsin-dependent but also depends on expression levels and cell type, we performed a detailed analysis of the spectral sensitivity of ChrimsonR-CA3 and CheRiff-CA1 pyramidal neurons (*SI Appendix*, Fig. S1). According to this spectral analysis, we selected 405 nm (1.2 mW mm^{-2}) to activate CheRiff-CA1 neurons and 625 nm (8 mW mm^{-2}) to activate ChrimsonR-CA3 neurons. These intensities reliably and selectively evoked single action potentials/spikes in CA3 or CA1 pyramidal neurons using 1-2 ms flashes after 7-10 days expression (Fig. 1B). Although 405 nm light partially activates ChrimsonR, it did not spike ChrimsonR-CA3 neurons at 1 mW mm^{-2} (depolarization 0-3 mV, Fig. 1B). Importantly, red light (625 nm) caused no photocurrents in CheRiff-CA1 neurons at intensities up to 100 mW mm^{-2} nor did the yellow epifluorescence light used to visualize mKate2 (*SI Appendix,* Fig. S1). Thus, by using only yellow light (see Materials and Methods) we never inadvertently depolarized the postsynaptic CheRiff-CA1 neurons (i.e. only during pairing were cultures exposed to wavelengths less than 565 nm).

Optogenetic induction of spike-timing-dependent plasticity

We recorded excitatory postsynaptic currents (EPSCs) in CheRiff- or non-transfected CA1 neurons (hereafter referred to as NT-CA1 neurons) while optogenetically stimulating the approximately 30 ChrimsonR-CA3 neurons with single orange (594 nm, 2 ms) light flashes at 20 s intervals. As CA3 was outside the field of view of the objective when we patched the CA1 pyramidal neurons, we coupled the orange laser through the condenser (Fig. 1C and D). After five minutes baseline, we switched from voltage- to current-clamp mode. Single presynaptic ChrimsonR-CA3 spikes (300 flashes at 5 Hz, 2 ms duration, see methods) led or followed spike bursts by about 10 ms in the CheRiff-CA1 postsynaptic neurons (3 flashes at 50 Hz, 2 ms duration, *SI Appendix,* Fig. S2).

Causal pairing (pre- before post-) induced tLTP (Fig, 1E, n = 12 experiments; p = 0.0002, Kolmogorov-Smirnov) whereas anti-causal pairing (post before pre) induced tLTD of ChrimsonR-CA3 to CheRiff-CA1 synapses (Fig. 1F, n = 11 experiments, p = 0.0009, Kolmogorov-Smirnov). There was a significant difference between causal and anti-causal groups (Fig 1G, p = 0.003, Kolmogorov-Smirnov). Importantly, the light stimulation used for causal pairing had no effect on synapses onto NT-CA1 neurons (median = 1.06, n = 6 experiments, p = 0.09, Kolmogorov-Smirnov, Fig 1G, *SI Appendix,* Fig. S2), indicating that oSTDP was specific to CheRiff-CA1 neurons and no plasticity was induced by the 5 Hz EPSPs alone. Evidently, using light to induce spikes in pre- and postsynaptic neurons produces oSTDP with similar timing rules as reported for this synapse when spikes were triggered by electrical stimulation (Bi and Poo, 1998; Debanne, Gähwiler and Thompson, 1998; Nevian and Sakmann, 2006; Wittenberg and Wang, 2006; Holbro *et al.*, 2010; Edelmann *et al.*, 2015; Tigaret *et al.*, 2016).

Having established that oSTDP induces both tLTP and tLTD during patch-clamp experiments, we then developed a no-patch method to induce oSTDP and read-out synaptic input strength days later. Illumination towers, containing independently controlled, collimated, red (630 nm) and violet (405 nm) high-power LEDs were constructed to stimulate ChrimsonR-CA3 and CheRiff-CA1 neurons in the incubator (Fig. 2A). As we could not record EPSPs and spikes in the incubator we used the immediate early gene cFos that is upregulated in burst-spiking neurons (Schoenenberger, Gerosa and Oertner, 2009) and in neurons that have undergone LTP (for review see Jaworski, Kalita and Knapska, 2018) as a surrogate. We found no cFos-positive ChrimsonR-CA3 neurons after causal pairing (9/9 slices) indicating that these neurons were not driven to burst by either the 630 nm light flashes (300 at 5 Hz, 8 mW mm^{-2}) or the 405 nm flashes (300 bursts of 3 at 50 Hz, 12 ms delay, 1 mW mm^{-2}). We validated this approach by observing that ChrimsonR-CA3 neurons expressed cFos when stimulated with bursts of three 630 nm flashes (300 bursts of 3 at 50 Hz, at 5 Hz, *SI Appendix,* Fig. S3) instead of single flashes. Thus, cFos is not expressed when pyramidal neurons fire 300 single spikes at 5 Hz but cFos is expressed in neurons firing 300 bursts of 3 spikes, i.e. the ChrimsonR-CA3 neurons were not burst firing during no-patch oSTDP induction.

Likewise, 83% of CheRiff-CA1 neurons expressed cFos indicating they were directly driven to fire bursts of spikes during causal pairing as expected (7 slices: 30/36 neurons; Fig. 2E**,** *SI Appendix*, Fig. S4). Importantly, whether NT-CA1 neurons expressed cFos depended critically on the number of ChrimsonR-CA3 neurons in the slice. In 5 slices with 36-53 ChrimsonR-CA3 neurons, no NT-CA1 neurons expressed cFos (Fig. 2E**,** *SI Appendix*, Fig. S4). In 2 slices with 60-61 ChrimsonR-CA3 neurons, some NT-CA1 neurons showed cFos staining, and in 2 slices with 96 or more ChrimsonR-CA3 neurons, cFos staining was evident throughout the entire CA1 (*SI Appendix*, Fig. S4). Thus, we adjusted the amount of ChrimsonR virus injected to transduce ~30 CA3 neurons (e.g. Fig 1A).

The cFos expression pattern after in-incubator causal pairing, indicated the CheRiff and ChrimsonR neurons were being stimulated as expected, so we looked at the outcome of oSTDP 3 days later. Since baseline synaptic strength cannot be directly assessed, we compared the strength of ChrimsonR-CA3 to CheRiff-CA1 synapses with the strength of synapses onto neighboring NT-CA1 neurons. ChrimsonR-CA3 neurons were spiked with 594 nm laser flashes as described above and EPSCs were sequentially recorded from at least one CheRiff- and at least three NT-CA1 neurons per slice (Fig. 3A, B). The input strength calculated for each CheRiff-CA1 neuron, is the average EPSC slope of the CheRiff-CA1 neuron divided by the slope of the combined average EPSC

recorded from the three or more NT-CA1 neurons in that slice (Fig. 3C). As expected, CheRiff-CA1 and neighboring NT-CA1 neurons received equivalent input from the ChrimsonR-CA3 neurons in control slices that were not previously stimulated with light, (Fig. 3D, no pairing; median = 0.91, mean = 1.04, CV = 0.53).

Input strength is potentiated three days after no-patch oSTDP

Three days after in-incubator causal pairing of EPSPs and spikes, the input strength from ChrimsonR-CA3 onto CheRiff-CA1 neurons was significantly stronger than in control 'no pairing' slices (Fig. 3D, +10 ms: median = 2.13, mean = 2.95, CV = 0.69; $P = 0.002$, Kolmogorov-Smirnov). Surprisingly, anti-causal pairing also resulted in stronger inputs three days later (Fig. 3D, -10 ms: median = 1.8, mean = 2.51, CV = 0.89; $P = 0.052$, Kolmogorov-Smirnov). The time interval between EPSPs and postsynaptic spikes was important, as input strength did not change significantly when Δt was 50 ms (Fig. 3D, +50 ms: median = 0.97, mean = 2.44, CV = 1.18; $P = 0.4$ Kolmogorov-Smirnov; -50 ms: median = 1.78, mean = 2.38, CV = 0.66; $P = 0.13$ Kolmogorov-Smirnov). Coincident activity of pre- and postsynaptic neurons was an absolute requirement for oSTDP as input strength was unchanged 3 days after burst firing the postsynaptic CheRiff-CA1 neurons alone (Fig. 3D, post only; $P = 0.6$ Kolmogorov-Smirnov). In previous studies, tLTP was associated with an immediate increase in postsynaptic excitability (Frick, Magee and Johnston, 2004; Debanne and Poo, 2010; Debanne, Inglebert and Russier, 2019). Three days after oSTDP, we found no differences in passive electrical parameters or excitability of CA1 neurons (*SI Appendix*, Fig. S5), indicating that the late effects of oSTDP were synaptic.

As for classical STDP (Bi and Poo, 1998; Debanne, Gähwiler and Thompson, 1998; Nevian and Sakmann, 2006; Edelmann *et al.*, 2015; Tigaret *et al.*, 2016), tLTP induced in the incubator was abolished when NMDA receptors were blocked during pairing (Fig. 3E, +CPP). Reducing the pairing frequency from 5 Hz to 0.1 Hz also prevented plasticity induction (Fig. 3E, 0.1 Hz), in line with previous studies (Wittenberg and Wang, 2006).

It was unexpected and intriguing that anti-causal pairing of pre- and postsynaptic spikes did not decrease the input strength (Fig. 3D). As the stimulation was repeated every 200 ms, the tested timings covered all possible phase shifts between pre- and postsynaptic activity (Fig. 3G). The absence of tLTD was particularly surprising because during patch-clamp recordings, causal and anti-causal oSTDP clearly had opposite effects on EPSCs (Fig. 1E-G). As the distribution of input strengths following anti-causal pairing (-10 ms) appeared rather bimodal, we tested pairing protocols of different length in an attempt to uncover the expected depression (Wittenberg and Wang, 2006). However, while 30 anti-causal pairings at 5 Hz did not induce any plasticity, all stronger protocols (100 to 500 repeats at 5 Hz) increased input strength (*SI Appendix*, Fig. S6).

We next investigated whether at a shorter time point after no-patch oSTDP, we would observe tLTD. As it takes time to settle the slices in the recording setup and sequentially patch the minimum of 4 neurons needed for one datapoint, the earliest time point after in-incubator oSTDP we could asses was 1-3 hours. Somewhat surprisingly, even at this earlier time, input strength was not significantly changed either by causal or anti-causal pairing, although a trend towards potentiation after causal pairing was apparent (*SI Appendix*, Fig. S7, -10 ms median = 1.04, $P = 0.2$ Kolmogorov-Smirnov; +10 ms median = 1.62, $P = 0.56$ Kolmogorov-Smirnov). Thus, tLTD was

observed only during patch-clamp recordings and not later when the CA1 neurons were not patched during oSTDP induction.

We were intrigued that the strength of causally paired CA3-CA1 connections seemed to increase in the days following plasticity induction. We reasoned that after oSTDP, circuits containing potentiated synapses might develop higher levels of spontaneous spiking in the incubator, increasing re-activation of the synapses between the paired CA3 and CA1 neurons (Sadowski, Jones and Mellor, 2016; Debanne, Inglebert and Russier, 2019). Thus, we globally increased activity by completely changing the slice culture medium 3-4 hours after oSTDP and suppressed activity by including tetrodotoxin in the fresh medium. Both manipulations prevented potentiation (Fig. 4). These results suggest that the synaptic memory of a short episode of coincident activity was actively maintained and amplified in the cultures, pointing to a process that requires replay of activity patterns in the selected circuits.

Discussion

In previous studies, the usual requirement of impaling the postsynaptic neuron with a sharp electrode or using whole-cell or perforated patch recordings to induce STDP, has made it impossible to assess the late (i.e. days later) effects of STDP. In the present study, we demonstrate that (1) the opsins CheRiff and ChrimsonR can be used to independently spike CA3 and CA1 neurons, (2) during patch-clamp recordings optogenetic causal pairing of pre- and postsynaptic spiking induces tLTP whereas anti-causal pairing induces tLTD, and (3) the long-term consequence of pairing closely apposed pre- and postsynaptic spikes is potentiation regardless of the timing sequence.

Since during short-term patch-clamp recordings, oSTDP follows the same timing rules as demonstrated in many studies of electrically-induced STDP (Markram *et al.*, 1997; Bi and Poo, 1998; Debanne, Gähwiler and Thompson, 1998; Meredith, Floyer-Lea and Paulsen, 2003; Zhang, Lau and Bi, 2009), we surmise that optically- and electrically-induced spiking are not fundamentally different. Causal pre before post pairing induces tLTP and anti-causal post before pre pairing induces tLTD. Late oSTDP is similar to short-term electrode-induced STDP in several important respects. Late oSTDP remains sensitive to spike timing, as no potentiation occurs when postsynaptic neurons spike 50 ms after the EPSP (Fig 3G). At this time, $GABA_A$ currents from feed-forward inhibition are strongly activated in CA1 neurons (Samulack and Lacaille, 1993) and may reduce the synaptic calcium influx necessary for potentiation as has been demonstrated for back-propagating action potentials (Marlin and Carter, 2014). Late tLTP also depends on NMDA receptors as is well established for electrode-induced STDP (Nevian and Sakmann, 2006), strongly suggesting that elevated intracellular [Ca^{2+}] in the postsynaptic neuron is essential. A further similarity of late oSTDP to electrode-induced STDP is the strong frequency-dependence of oSTDP (Wittenberg and Wang, 2006): At a pairing repetition rate of 5 Hz, tLTP was observed, but not when the pairing rate was reduced to 0.1 Hz.

To us, the most surprising result is the apparent lack of tLTD three days after oSTDP induction. None of the manipulations we performed; increasing or decreasing the number of anti-causal pairing repetitions, changing the pairing interval or decreasing the pairing frequency unmasks a late tLTD. Nor was tLTD apparent at the earliest time window (1-3 hours) feasible after no-patch oSTDP. The fact that we did not detect statistically significant differences in input strength at this early time point is consistent with a slow, activity-dependent enhancement of tLTP. We hypothesize

that slight differences in synaptic strength or excitability, induced by the only structured activity that was ever provided in these slice cultures, were enhanced over time by an active process. That the 'memory' of causal pairing is erased when spontaneous activity is disrupted supports this hypothesis, but obtaining direct evidence will require the continuous monitoring of the circuit activity over several days. Interestingly, maintenance and consolidation of memories also appear to require ongoing activity and NMDA receptors (Shimizu *et al.*, 2000; Cui *et al.*, 2004). Transient knock-out of NMDA receptors wipes out previously encoded memory but does not prevent the future acquisition of new memories (Cui *et al.*, 2004).

In addition to time of readout, there are other considerations for comparing the early and late outcome of the oSTDP experiments. The temperature of the slices during the induction were different, 33 °C vs 37 °C. While we performed the early oSTDP patch-clamp experiments in slice culture medium, we had to omit the horse serum, which was present in the medium during incubator stimulation. Probably the most important difference is that in early oSTDP experiments, the postsynaptic neurons had whole-cell patch-clamp electrodes attached. Might it be that tLTD occurs at the -10 ms timing interval only in 'damaged' neurons with contents being dialyzed with recording electrodes? We induced oSTDP 5-10 minutes after obtaining whole-cell access, as it is well known that washout of important cellular components prevents LTP induction (Malinow and Tsien, 1990). Evidence against the hypothesis that early tLTD is purely due to washout are STDP studies using sharp electrodes or perforated patch recordings, that have reported both tLTD and tLTP (Meredith, Floyer-Lea and Paulsen, 2003; Zhang, Lau and Bi, 2009). Still, it is possible that the act of patching the postsynaptic neuron compromises tLTP, and biases synapses towards depression (Sjöström, Turrigiano and Nelson, 2001). Indeed, Pang et al., who used extracellular electrodes to induce and record STDP failed to observe LTD at early (< 30 min) time points. Thirty minutes after pairing single pre and postsynaptic stimuli they observed LTP for not only causal pairing intervals of 0 to +40 ms but also after anti-causal pairing of -10 ms. During their 4 hour recordings LTP, persisted for timings from -10 ms to 20 ms and LTD slowly appeared only for the anti-causal pairing interval of -20 ms. Perhaps our choice of triplet spikes in the postsynaptic neurons prevented the later appearance of tLTD or that at even later time points the change in sign from LTD to LTP occurs. However, both this and our study show that the late LTD window following STDP is much reduced compared to short-term patch or sharp electrode recordings. Thus, STDP has hitherto unappreciated slow dynamics that should be taken into consideration in future models of synaptic memory.

What if the opsin expressing neurons either failed to fire action potentials during no-patch oSTDP induction or fired multiple action potentials? Extensive experience has taught us that very short (1-2 ms) light flashes with an intensity range from threshold until about 5x spike threshold will reliably evoke single spikes in neurons expressing relatively fast channelrhodopsins. To induce oSTDP we therefore used very short flashes of calibrated intensity set to ~2x the average spike threshold determined for CheRiff-CA1 and ChrimsonR-CA3 neurons, which was constant from 7 to 12 days after transfection. Additionally, we verified during oSTDP readout that every CheRiff-CA1 neuron analyzed indeed spiked at this intensity (see methods). Fewer than 5% of all CheRiff-CA1 neurons failed to spike at this intensity and were discarded. Of the remaining CheRiff-CA1 neurons, only 6% fired two spikes to the single light flash. On the presynaptic side, we selected the lowest light intensity tested that evoked at least -20 pA EPSCs in the non-transfected neurons, to bias the synapses being assayed toward those made by ChrimsonR-CA3 neurons with low spike thresholds i.e. those synapses most likely being activated in the incubator. The cFos staining results

demonstrate that CA3 stimulation does not driving bursting throughout CA1 as long as fewer than 50 CA3 neurons are transduced, and that the CheRiff neurons burst during oSTDP induction. That the early effects of oSTDP replicated the classical asymmetric STDP window, strongly argues against optogenetic artifacts being solely responsible for the difference in early and late effects. As channelrhodopsins are distributed in the plasma membrane, it could even be argued that optical generation of spikes is more physiological than somatic current injection; spiking normally arises from distributed synaptically-induced depolarization of dendrites and spines. Indeed, experiments pairing mossy fiber stimulation with CA3-CA3 synaptic inputs induces tLTP or tLTD of the CA3-CA3 synapses without spiking of the postsynaptic CA3 neuron (Brandalise and Gerber, 2014). Likewise, at CA3-CA1 Schaffer collateral synapses tLTP can occur without postsynaptic spikes (Hardie and Spruston, 2009). Thus, if CheRiff-CA1 cells occasionally missed spiking and only depolarized in response to the violet light flashes, tLTD and tLTP would still be the expected outcome.

While the majority of STDP studies report both potentiation and depression, 'LTP-only' STDP windows have been observed at human hippocampal, human and rat neocortical synapses (Testa-Silva, 2010; Brzosko, Schultz and Paulsen, 2015) and in mouse hippocampus (Wittenberg and Wang, 2006), most commonly in the presence of increased dopamine (Zhang, Lau and Bi, 2009; Brzosko, Schultz and Paulsen, 2015). If presynaptic activity is paired with prolonged postsynaptic bursts (plateau potentials), the timing window for Schaffer collateral potentiation can be extended to several seconds in the causal and anti-causal direction (Bittner *et al.*, 2017). Explanations for these discrepant outcomes of early oSTDP abound, but we speculate that if synaptic strength was assessed after several days, the outcome of repeated coincident activity may always be potentiation regardless of the exact temporal sequence. Low frequency LTD might reflect a mechanism to prevent runaway potentiation. And conservation of total synaptic weight may be provided by heterosynaptic LTD or via generalized downscaling processes (Turrigiano, 2017). As the post oSTDP synaptic input strength was always compared to the synaptic strength from the same presynaptic neurons onto close neighbors, we cannot determine whether the overall synaptic strength might have increased over the three days. Understanding better the dynamics of synaptic strength following STDP and how ongoing activity influences the stability of late tLTP will certainly influence our understanding of how and if memory storage is related to synaptic plasticity.

Materials and Methods

Rat organotypic hippocampal slice cultures

Wistar rats were housed and bred at the University Medical Center Hamburg-Eppendorf (UKE) animal facility and sacrificed according to German Law (Tierschutzgesetz der Bundesrepublik Deutschland, TierSchG) with approval from the Behörde für Gesundheit und Verbraucherschutz Hamburg and the animal care committee of the UKE. The procedure for organotypic cultures was modified from Stoppini et al. (Stoppini, Buchs and Muller, 1991), using media without antibiotics. Detailed protocol was previously published in (Gee *et al.*, 2017). After opsins were expressing, great care was taken to protect the cultures from wavelengths of light below 560 nm to prevent unintentional co-activation of ChrimsonR and CheRiff-expressing neurons. Handling and normal medium changes (2/3, twice per week) were under dim yellow light, which may directly depolarize ChrimsonR but not CheRiff expressing neurons (Osram LUMILUX CHIP control T8).

Viral vector-based transduction

The plasmid pAAV-syn-ChrimsonR-TdTomato, a kind gift from Edward Boyden (Addgene # 59171), was packaged into AAV viral particles with serotype Rh10 (7.22×10^{13} vg ml^{-1}) at the Vector Core facility of the University Medical Center Hamburg-Eppendorf. One µl was loaded into a micropipette with the tip broken to ~10 µm diameter. Slice cultures (12-14 DIV) were transferred into sterile pre-warmed (37 °C) HEPES-buffered solution containing: NaCl (145 mM, Sigma; S5886-500G), HEPES (10 mM, Sigma; H4034-100G), D-glucose (25 mM, Sigma; G7528-250G), KCl (2.5 mM, Fluka; 60121-1L), $MgCl_2$ (1 mM, Fluka; 63020-1L), $CaCl_2$ (2 mM, Honeywell; 21114-1L), pH 7.4, 318 mOsm kg^{-1}. The virus-containing pipette was inserted into CA3 and a small bolus was pressure-ejected using 3-5 pressure pulses (Picospritzer: 2 bar, 80-100 ms). Our aim was to transduce approximately 30 CA3 neurons with ChrimsonR. A detailed description of the viral transduction has been published (J. Simon Wiegert, Gee and Oertner, 2017).

Single-cell electroporation

Plasmids used for electroporation were: 1) pAAV-hsyn-CheRiff-eGFP (Addgene #51697), 0.5 ng ml^{-1}, kindly provided by Adam Cohen; 2) pCI-syn-mKate2, 10 ng ml^{-1} was created by replacing GCaMP3 in pCI-syn-GCaMP3 using hindIII and NotI with mKate2-N from pmKate2-N (Evrogen cat. # FP182). Plasmids were diluted in intracellular solution containing: K-gluconate (135 mM, Sigma; G4500-100G), EGTA (0.2 mM, Sigma-Aldrich; E0396-10G), HEPES (10 mM, Sigma; H4034-100G), $MgCl_2$ (4 mM, Fluka; 63020-1L), Na_2-ATP (4 mM, Aldrich; A26209-1G), Na-GTP (0.4 mM, Sigma; G8877-100MG), Na_2-phosphocreatine (10 mM, Sigma; P7936-1G), ascorbate (3 mM, Sigma; A5960-100G), pH 7.2, 295 mOsm kg^{-1}. Slice cultures were transferred to a sterile microscope chamber filled with sterile 37°C HEPES-buffered solution (see viral vector-based transduction) either right after AAV injection or 1 day later. Pipettes (10-15 MΩ, World Precision Instruments; TW150F-3) were filled with the plasmid mixture and several pyramidal neurons in CA1 were touched and electroporated using an Axoporator (25 pulses, -12 V, 500 µs, 50 Hz). A detailed description of the electroporation procedure has been published (J Simon Wiegert, Gee and Oertner, 2017).

CheRiff and ChrimsonR characterization

For characterizing responses to multiple wavelengths, we used a pE-4000 CoolLED (CoolLED Ltd., s/n CP0180) with an additional filter for 550 nm (555 ± 20 nm) coupled through the dual camera port of the electrophysiology setup described below. Light intensities in the specimen plane were measured using a 918D-ST-UV sensor and 1936R power meter (Newport). Light flashes (1 ms, low to high intensity) were delivered every 20 s with one minute between wavelength sequences. Whole cell currents were recorded (see electrophysiology below) with synaptic transmission and action potentials blocked by CPPene (10 µM, Tocris bioscience; 1265), NBQX (10 µM, Tocris bioscience; 1044), picrotoxin (100 µM, Sigma; P1675-1G) and tetrodotoxin (1 µM, HelloBio; HB1035). Seven CA1 (CheRiff) and eleven CA3 (ChrimsonR) neurons were recorded from to obtain n = 4 responses at each wavelength/intensity combination. Average peak light-evoked currents were determined and plotted (*SI Appendix*, Fig. S1) using a self-written MATLAB code.

Electrophysiology and optogenetic stimulation

The setup is based on an Olympus BX61WI microscope fitted with Dodt contrast, epifluorescence and CCD-camera (DMK23U274, The Imaging Source) on a dual camera port (see Fig. 1C). For light stimulation through the objective an LED combiner (Mightex Systems, wavelengths 625, 530,

470, 405 nm) was coupled via 1 mm multimode fiber and collimator (Thorlabs) mounted on one of the camera ports. A 40x water immersion objective (Plan-Apochromat 1.0 NA DIC VIS-IR, Zeiss, illuminated field ø 557 µm) or a 10x water immersion objective (UMPlanFL 0.30 NA W, Olympus, illuminated field ø 2.65 mm) were used. Light intensities through the objectives were measured in the specimen plane using a calibrated power meter (LaserCheck, Coherent or 918D-ST-UV sensor / 1936R power meter, Newport). To locally activate CA3 neurons, the orange (594) laser beam of an Omicron Light Hub was coupled to an optical fiber fitted with a collimator (Thorlabs) mounted on a lockable swing arm. This construction allowed us to point the laser beam at different angles through the center of the back aperture of the oil immersion condenser (NA 1.4, Olympus) to locally illuminate neurons in CA3 away (~1.5 mm) from the optical axis, with high intensity and little light scattering (Fig 1C). After final laser positioning, the stage was not moved and CA1 neurons within the single field of view were recorded from.

Whole-cell patch-clamp recordings were performed using an Axopatch 200B (Axon Instruments, Inc.) amplifier, National Instruments A/D boards and Ephus software (Suter *et al.*, 2010). All recordings, except the experiments in Fig. 1E-G and 2B-D (see next section), were performed blind to slice treatment at 30°C (in-line heater, Warner Instruments) in artificial cerebral spinal fluid containing: NaCl (119 mM, Sigma; S5886-500G), $NaHCO_3$ (26.2 mM, Sigma; S5761-500G), D-glucose (11 mM, Sigma; G7528-250G), KCl (2.5 mM, Fluka; 60121-1L), NaH_2PO_4 (1 mM, Sigma; S5011-100G), $MgCl_2$ (4 mM, Fluka; 63020-1L), $CaCl_2$ (4 mM, Honeywell; 21114-1L), pH 7.4, ~310 mOsm kg^{-1}, saturated with humidified 95% O_2 / 5% CO_2. Patch electrodes (3-4 MΩ, World Precision Instruments; 1B150F-3) were filled with the same intracellular solution used for electroporation (above). Liquid junction potential was measured (-14.1 to -14.4 mV) and corrected. CA1 pyramidal neurons were patched under the 40x water immersion objective and voltage-clamped at -70 mV (LJP corrected). A test pulse (-5 mV, 200 ms) was applied at the start of every sweep. Series resistance (Rs) was less than 20 MΩ, did not change more than 30% and was not compensated in voltage clamp. In current clamp we used the bridge balance compensation.

Optogenetic induction of spike-timing dependent plasticity during whole-cell recordings

Eight to eleven days after virus injection and electroporation of ChrimsonR and CheRiff, slices were transferred to the electrophysiology setup and perfused with slice culture medium (described above) without horse serum (replaced with MEM), supplemented with D-serine (30 µM, Tocris Bioscience; 0226) and diluted slightly to give ~308 mOsm kg^{-1} (33 °C, saturated with humidified 95% O_2 / 5% CO_2). The LJP was measured and corrected (-15.3 mV). The medium (50 ml) was recycled during the experiment and changed every 4 hours or every 4 slices, whichever came first. With the 594 nm laser positioned to stimulate ChrimsonR-CA3 neurons, a CA1 neuron was patched and EPSCs were recorded (every 20s) at -65.3 mV (LJP corrected) where inhibitory currents were clearly outward. Laser intensity was set to evoke EPSCs of approximately -100 pA (range -50 pA to -200 pA). Baseline EPSCs were recorded for up to 5 minutes after break-in. The 10x objective was carefully moved into position to maximize the area of the slice illuminated and the amplifier was switched to current clamp to allow spiking of the CA1 neuron during paired optogenetic stimulation. To induce plasticity, stimulation of ChrimsonR-CA3 neurons 300 x 2 ms pulses at 5 Hz (594 nm laser at baseline intensity plus simultaneous red LED stimulation in the CA1 (625 nm, 2 mW mm^{-2})) was combined with bursts of 3 violet LED stimuli in CA1 (405 nm, 2 ms, 50 Hz, 1 mW mm^{-2}) to activate CheRiff-CA1 neurons. We set the delay between orange/red and the last or first of the violet light flashes of -10 ms or +10 ms for anti-causal and causal pairing, respectively but after 9 experiments observed the actual median delay from the last action potential (AP) to EPSP onset was -14.2 ms during anti-causal pairing and from EPSP onset to the first AP was 6.8 ms

during causal pairing. We therefore advanced the red/orange flash by 2 ms relative to the violet flash during the remaining experiments obtaining a more symmetrical median timing of -12.4 ms during anti-causal and 8.8 ms during causal pairing. After pairing CA3 and CA1 stimulation, EPSCs (0.05 Hz orange laser flashes) were recorded for an additional 25 minutes. The EPSC slope was measured using a self-written script in MATLAB. To determine whether tLTP or tLTD occurred in an individual experiment the baseline slopes (black points in Fig. 1E) and the slopes measured in the last 5 minutes (magenta points in Fig. 1E) were compared with Kolmogorov-Smirnov tests (significance $p < 0.05$). A Kolmogorov-Smirnov test was used to test whether the normalized EPSC slopes were different between the anti-causal and causally paired groups. Plots and statistical analyses were performed using MATLAB and GraphPad Prism.

In-incubator oSTDP, read-out and analysis

For all 'no patch' oSTDP experiments, read-out and analysis were performed by an investigator blinded to the induction protocol. Unblinding occurred after the target n for a particular group was reached (~ 7 CheRiff neurons from 4 slices). Experimental groups were inter-mixed to ensure blinding and to mitigate the possibility of unexpected batch or time-dependent factors influencing the outcome resulting in uneven n's between treatment groups.

We waited 7-10 days to allow stable expression of ChrimsonR and CheRiff. One to three days before in-incubator light stimulation, the slice cultures (placed singly on the inserts) were transferred to and centered in a 35 mm culture dish. Where indicated CPPene (1 µM, Fig. 3E) was added to the slice culture medium the day before. The closed petri dish containing the centered slice culture was placed in an LED illumination tower constructed from 30 mm optical bench parts (Thorlabs) that was inside a dedicated incubator (Fig. 2A). The tower contained an injection-molded reflector (Roithner LaserTechnik, 10034) to collimate the 630 nm LED (Cree XP-E red) and an aspheric condenser lens (Thorlabs ACL2520U-A) to collimate the 405 nm LED (Roschwege Star-UV405-03-00-00). The LEDs were powered and controlled from outside the incubator by a two-channel Grass S8800 stimulator, two constant-current drivers (RECOM RCD-24-1.20) and a timer. LED power was adjusted to give 1.2 mW mm^{-2} for 405 nm and 8 mW mm^{-2} for 630 nm inside the petri dish in the specimen plane. Considering the spread in actual spike-burst delay (Fig. 1G), Δt was set to +52, +12, -8, or -48 ms to produce EPSP-spike delays of ~+50 ms, +10 ms, -10 ms and -50 ms, respectively (light pulse duration 2 ms). Pairing frequency was 5 Hz or 0.1 Hz. Paired activation was repeated 300 times unless otherwise indicated. 'Non-paired' cultures were handled identically but no light stimulation was given. After pairing, each petri dish was marked with only a letter code and date/time of pairing. Where indicated (Fig. 4), 3-4 hours after pairing fresh pre-warmed medium with 1 µM tetrodotoxin (TTX) was pipetted on top of the membrane to immediately silence neurons in the slice. The medium under the slice was then aspirated, replaced with the TTX containing medium and the medium on top of the slice was removed before returning the slice to the incubator, so that the slice was again exposed to the humidified incubator atmosphere. Two days later the TTX was washed 3 times with fresh medium and the slices returned to the incubator until the following day when they were recorded from. For the medium change condition, cultures were handled identically except the medium never contained TTX.

One hour or 3 days after in-incubator stimulation, slices were transferred by the blinded investigator to the electrophysiology setup with on/off axis stimulation and perfused with ACSF at 30 °C as described above. The slice was positioned so that CheRiff-CA1 neurons as well as at least 5 non-transfected CA1 pyramidal neurons were in the field of view of the 40x objective and camera (Fig. 3A). The 594 nm laser was positioned to activate the ChrimsonR-CA3 neurons (see above). Whole-cell patch-clamp recordings were sequentially made from 3 to 4 NT-CA1 pyramidal neurons and 1 to 5 CheRiff-CA1 pyramidal neurons in a pseudo-random sequence without moving the stage to

ensure constant CA3 stimulation (holding potential -70 mV to ensure separation between EPSCs and IPSCs). While still in cell-attached mode, CA1 neurons were illuminated with a single 405 nm light flash (1 ms, 1.2 mW mm^{-2}). None of the 250 NT-CA1 neurons spiked. Of 212 fluorescent CheRiff-CA1 neurons, 96% spiked in response to the violet flash, 190 fired a single spike (89.6%) and 13 fired 2-3 spikes (6.1%). The recordings were immediately discontinued from the remaining 9 neurons that did not spike (4.25%).

After break-in, orange laser flashes (594 nm, 20 s interval) stimulated ChrimsonR-CA3 neurons to evoke EPSCs in the CA1 neurons. EPSC onset was typically 6 to 8 ms after the stimulation. If the delay to EPSC onset was 13 ms or longer they were assumed polysynaptic and not analyzed. Ten EPSCs were recorded at each of 3 laser intensities from each CA1 neuron (when spontaneous events obscured the EPSCs a few more sweeps were collected). The middle intensity was set to evoke an EPSC of about -100 to -300 pA in the first recording from a given slice. The same 3 intensities were used for all neurons in a given slice. Importantly, we found no correlation between laser intensity and the amount of LTP induced. At the end of each recording, we injected a series of current steps to assess cellular excitability. Cells without pyramidal-like firing patterns (i.e. high AP frequency, large amplitude after-hyperpolarization) were eliminated from the analysis.

For analysis, we selected the EPSCs from one laser intensity per slice. The selected intensity evoked the most similar EPSC slopes that were at least 20 pA in three non-transfected cells (usually the lowest laser intensity). Individual sweeps with spontaneous EPSCs/IPSCs within 10 ms of the stimulation were suppressed. If fewer than 4 sweeps remained at the selected laser intensity, the recording was discarded. A custom Matlab routine averaged the EPSCs, detected the (first) peak and the 20-60% slope (Fig. 3C). If the time of the peak varied by more than 5 ms between neurons, we suspected a mixture of mono and polysynaptic responses and the slice was excluded. Input strength was defined as the slope from each CheRiff-CA1 neuron divided by the slope of the average EPSC from all NT-CA1 neurons in the given slice. GraphPad Prism 8 was used for statistics and to create plots.

Immunohistochemistry

Ninety minutes after stimulation, slices were fixed (30 minutes, ice-cold 4% paraformaldehyde in PBS). Slices were washed in PBS (3 x 10 min) and blocked (2 hours 5% donor horse serum, 0.3 % TritonTM X-100 in PBS at RT) and then incubated overnight with the primary antibody (4° C, rabbit anti-cFos, Santa Cruz Biotechnology, Inc., sc-52, 1:500) in carrier solution (1 % Bovine serum albumin, 0.3 % TritonTM X-100 in PBS). Next day slices were washed 3 times in PBS and incubated at RT for 2 hours with a secondary antibody (Alexa Fluor 488 goat anti-rabbit, Life Technologies, A11008; or Alexa Fluor 568 goat anti-rabbit, Life Technologies, A11011) at 1:1000 in carrier solution (same as above) and afterwards washed again (3 x 10 min) in PBS and mounted with Shandon Immu-Mount (Thermo Scientific; 9990402).

Confocal microscopy

An Olympus F1000 confocal microscope and 20x objective (UPLSAPO 0.85 NA, Olympus) were used with the laser/filter sets designed for Alexa 488, Alexa 546 and Alexa 568 as appropriate. Z-series images were obtained using a 3 µm z-step at a 1024x1024-pixel resolution scanning at 12.5 µs per pixel. Image parameters were adjusted for the red and green channels and were kept constant throughout. Fiji/ImageJ (Schindelin *et al.*, 2012) was used to project the z-series and overlay channels.

Acknowledgments

We would like to thank Mark van Rossum for critically reading the manuscript. Iris Ohmert, Sabine Graf, Torsten Renz, Dirk Lubrich, Lennart Sobirey, Paul Lamothe and Ingke Braren (UKE Vector facility) provided important technical support. CheRiff was a gift from Adam Cohen, ChrimsonR was a gift from Edward Boyden. The first spectral characterization of ChrimsonR-expressing neurons in slice cultures was performed by Katie Ferguson and Longzhi Tan during the 2014 Neurobiology Course at MBL in Woods Hole. Funding was received from: the Landesforschungsförderung Hamburg; the Deutsche Forschungsgemeinschaft (DFG) grants SPP 1665 220176618, SPP1926 315380903, SFB 936 178316478, SFB 1328 335447717, FOR 2419 278170285, Emmy Noether 259979908 and the European Research Council (ERC-StG 714762).

References

Adamantidis, A. R. *et al.* (2007) 'Neural substrates of awakening probed with optogenetic control of hypocretin neurons', *Nature*, 450(7168), pp. 420–424. doi: 10.1038/nature06310.

Barria, A. *et al.* (1997) 'Regulatory phosphorylation of AMPA-type glutamate receptors by CaM-KII during long-term potentiation.', *Science (New York, N.Y.)*, 276(5321), pp. 2042–5. doi: 10.1126/science.276.5321.2042.

Bi, G. and Poo, M. (1998) 'Synaptic Modifications in Cultured Hippocampal Neurons: Dependence on Spike Timing, Synaptic Strength, and Postsynaptic Cell Type', *The Journal of Neuroscience*, 18(24), pp. 10464–10472. doi: 10.1523/JNEUROSCI.18-24-10464.1998.

Bittner, K. C. *et al.* (2017) 'Behavioral time scale synaptic plasticity underlies CA1 place fields.', *Science (New York, N.Y.)*, 357(6355), pp. 1033–1036. doi: 10.1126/science.aan3846.

Bliss, T. V and Lomo, T. (1973) 'Long-lasting potentiation of synaptic transmission in the dentate area of the anaesthetized rabbit following stimulation of the perforant path.', *The Journal of physiology*, 232(2), pp. 331–56. doi: 10.1113/jphysiol.1973.sp010273.

Boyden, E. S. *et al.* (2005) 'Millisecond-timescale, genetically targeted optical control of neural activity', *Nature Neuroscience*, 8(9), pp. 1263–1268. doi: 10.1038/nn1525.

Brandalise, F. and Gerber, U. (2014) 'Mossy fiber-evoked subthreshold responses induce timing-dependent plasticity at hippocampal CA3 recurrent synapses', *Proceedings of the National Academy of Sciences*, 111(11), pp. 4303–4308. doi: 10.1073/pnas.1317667111.

Brzosko, Z., Schultz, W. and Paulsen, O. (2015) 'Retroactive modulation of spike timing-dependent plasticity by dopamine.', *eLife*, 4, p. e09685. doi: 10.7554/eLife.09685.

Costa, R. P. *et al.* (2015) 'Unified pre- and postsynaptic long-term plasticity enables reliable and flexible learning', *eLife*. doi: 10.7554/eLife.09457.

Cui, Z. *et al.* (2004) 'Inducible and Reversible NR1 Knockout Reveals Crucial Role of the NMDA Receptor in Preserving Remote Memories in the Brain', *Neuron*, 41(5), pp. 781–793. doi: 10.1016/S0896-6273(04)00072-8.

Debanne, D., Gähwiler, B. H. and Thompson, S. M. (1998) 'Long-term synaptic plasticity between pairs of individual CA3 pyramidal cells in rat hippocampal slice cultures.', *Journal of Physiology*, 507(1), pp. 237–247. doi: 10.1111/j.1469-7793.1998.237bu.x.

Debanne, D., Inglebert, Y. and Russier, M. (2019) 'Plasticity of intrinsic neuronal excitability', *Current Opinion in Neurobiology*, 54, pp. 73–82. doi: 10.1016/j.conb.2018.09.001.

Debanne, D. and Poo, M.-M. (2010) 'Spike-timing dependent plasticity beyond synapse - pre- and

post-synaptic plasticity of intrinsic neuronal excitability.', *Frontiers in synaptic neuroscience*, 2, p. 21. doi: 10.3389/fnsyn.2010.00021.

Diamond, A., Schmuker, M. and Nowotny, T. (2019) 'An unsupervised neuromorphic clustering algorithm', *Biological Cybernetics*, 113(4), pp. 423–437. doi: 10.1007/s00422-019-00797-7.

Doyère, V. *et al.* (1996) 'Low-frequency trains of paired stimuli induce long-term depression in area CA1 but not in dentate gyrus of the intact rat', *Hippocampus*, 6(1), pp. 52–57. doi: 10.1002/(SICI)1098-1063(1996)6:1<52::AID-HIPO9>3.0.CO;2-9.

Edelmann, E. *et al.* (2015) 'Theta Burst Firing Recruits BDNF Release and Signaling in Postsynaptic CA1 Neurons in Spike-Timing-Dependent LTP', *Neuron*. Cell Press, 86(4), pp. 1041–1054. doi: 10.1016/j.neuron.2015.04.007.

Frey, U., Huang, Y. and Kandel, E. (1993) 'Effects of cAMP simulate a late stage of LTP in hippocampal CA1 neurons', *Science*, 260(5114), pp. 1661–1664. doi: 10.1126/science.8389057.

Frick, A., Magee, J. and Johnston, D. (2004) 'LTP is accompanied by an enhanced local excitability of pyramidal neuron dendrites.', *Nature neuroscience*, 7(2), pp. 126–135. doi: 10.1038/nn1178.

Gee, C. E. *et al.* (2017) 'Preparation of Slice Cultures from Rodent Hippocampus.', *Cold Spring Harbor protocols*, 2017(2), pp. 126–130. doi: 10.1101/pdb.prot094888.

Gerstner, W. *et al.* (1996) 'A neuronal learning rule for sub-millisecond temporal coding.', *Nature*, 383(6595), pp. 76–81. doi: 10.1038/383076a0.

Hardie, J. and Spruston, N. (2009) 'Synaptic Depolarization Is More Effective Than Back-Propagating Action Potentials During Induction of Associative Long-Term Potentiation in Hippocampal Pyramidal Neurons', *Journal of Neuroscience*. J Neurosci, 29(10), pp. 3233–3241. doi: 10.1523/JNEUROSCI.6000-08.2009.

Hayashi, Y. *et al.* (2000) 'Driving AMPA receptors into synapses by LTP and CaMKII: requirement for GluR1 and PDZ domain interaction.', *Science (New York, N.Y.)*, 287(5461), pp. 2262–7. doi: 10.1126/science.287.5461.2262.

Hochbaum, D. R. *et al.* (2014) 'All-optical electrophysiology in mammalian neurons using engineered microbial rhodopsins', *Nature Methods*, 11(8), pp. 825–833. doi: 10.1038/nmeth.3000.

Holbro, N. *et al.* (2010) 'AMPA receptors gate spine Ca(2+) transients and spike-timing-dependent potentiation', *Proc Natl Acad Sci U S A*. 2010/08/28, 107(36), pp. 15975–15980. doi: 10.1073/pnas.1004562107.

Huber, D. *et al.* (2008) 'Sparse optical microstimulation in barrel cortex drives learned behaviour in freely moving mice.', *Nature*, 451(7174), pp. 61–4. doi: 10.1038/nature06445.

Jaworski, J., Kalita, K. and Knapska, E. (2018) 'c-Fos and neuronal plasticity: the aftermath of Kaczmarek's theory.', *Acta neurobiologiae experimentalis*, 78(4), pp. 287–296. doi: 10.21307/ane-2018-027.

Klapoetke, N. C. *et al.* (2014) 'Independent optical excitation of distinct neural populations.', *Nature methods*, 11(3), pp. 338–46. doi: 10.1038/nmeth.2836.

Malenka, R. C. *et al.* (1989) 'An essential role for postsynaptic calmodulin and protein kinase activity in long-term potentiation.', *Nature*, 340(6234), pp. 554–7. doi: 10.1038/340554a0.

Malinow, R. and Tsien, R. W. (1990) 'Presynaptic enhancement shown by whole-cell recordings of long-term potentiation in hippocampal slices', *Nature*, 346(6280), pp. 177–180. doi: 10.1038/346177a0.

Markram, H. *et al.* (1997) 'Regulation of synaptic efficacy by coincidence of postsynaptic APs and EPSPs', *Science*, 275, pp. 213–215. doi: 10.1126/science.275.5297.213.

Marlin, J. J. and Carter, A. G. (2014) 'GABA-A receptor inhibition of local calcium signaling in spines and dendrites.', *The Journal of neuroscience : the official journal of the Society for Neuroscience*. J Neurosci, 34(48), pp. 15898–911. doi: 10.1523/JNEUROSCI.0869-13.2014.

Masquelier, T., Guyonneau, R. and Thorpe, S. J. (2009) 'Competitive STDP-Based Spike Pattern Learning', *Neural Computation*, 21(5), pp. 1259–1276. doi: 10.1162/neco.2008.06-08-804.

Meredith, R. M., Floyer-Lea, A. M. and Paulsen, O. (2003) 'Maturation of long-term potentiation induction rules in rodent hippocampus: role of GABAergic inhibition.', *Journal of Neuroscience*, 23(35), pp. 11142–11146. doi: 10.1523/jneurosci.23-35-11142.2003.

Mozafari, M. *et al.* (2019) 'SpykeTorch: Efficient Simulation of Convolutional Spiking Neural Networks With at Most One Spike per Neuron.', *Frontiers in Neuroscience*. Front Neurosci, 13, p. 625. doi: 10.3389/fnins.2019.00625.

Nagel, G. *et al.* (2003) 'Channelrhodopsin-2, a directly light-gated cation-selective membrane channel', *Proceedings of the National Academy of Sciences*, 100(24), pp. 13940–13945. doi: 10.1073/pnas.1936192100.

Nevian, T. and Sakmann, B. (2006) 'Spine Ca2+ Signaling in Spike-Timing-Dependent Plasticity', *Journal of Neuroscience*, 26(43), pp. 11001–11013. doi: 10.1523/JNEUROSCI.1749-06.2006.

Pang, K. K. L. *et al.* (2019) 'Long-term population spike-timing-dependent plasticity promotes synaptic tagging but not cross-tagging in rat hippocampal area CA1', *Proceedings of the National Academy of Sciences*, 116(12), pp. 5737–5746. doi: 10.1073/pnas.1817643116.

Parvez, S., Ramachandran, B. and Frey, J. U. (2010) 'Functional differences between and across different regions of the apical branch of hippocampal CA1 dendrites with respect to long-term depression induction and synaptic cross-tagging.', *Journal of Neuroscience*, 30(14), pp. 5118–23. doi: 10.1523/JNEUROSCI.5808-09.2010.

van Rossum, M. C., Bi, G. Q. and Turrigiano, G. G. (2000) 'Stable Hebbian learning from spike timing-dependent plasticity.', *Journal of Neuroscience*, 20(23), pp. 8812–8821. doi: 10.1523/jneurosci.20-23-08812.2000.

Sadowski, J. H. L. P., Jones, M. W. and Mellor, J. R. (2016) 'Sharp-Wave Ripples Orchestrate the Induction of Synaptic Plasticity during Reactivation of Place Cell Firing Patterns in the Hippocampus', *Cell Reports*. Cell Press, 14(8), pp. 1916–1929. doi: 10.1016/J.CELREP.2016.01.061.

Samulack, D. D. and Lacaille, J.-C. (1993) 'Hyperpolarizing synaptic potentials evoked in CA1 pyramidal cells by glutamate stimulation of interneurons from the oriens/alveus border of rat hippocampal slices. II. sensitivity to GABA antagonists', *Hippocampus*, 3(3), pp. 345–358. doi: 10.1002/hipo.450030309.

Schindelin, J. *et al.* (2012) 'Fiji: an open-source platform for biological-image analysis', *Nature Methods*, 9(7), pp. 676–682. doi: 10.1038/nmeth.2019.

Schoenenberger, P., Gerosa, D. and Oertner, T. G. (2009) 'Temporal control of immediate early

gene induction by light.', *PLoS ONE*, 4(12), p. e8185. doi: 10.1371/journal.pone.0008185.

Serrano-Gotarredona, T. *et al.* (2013) 'STDP and STDP variations with memristors for spiking neuromorphic learning systems', *Frontiers in Neuroscience*, 7. doi: 10.3389/fnins.2013.00002.

Shimizu, E. *et al.* (2000) 'NMDA receptor-dependent synaptic reinforcement as a crucial process for memory consolidation.', *Science (New York, N.Y.)*, 290(5494), pp. 1170–4. doi: 10.1126/science.290.5494.1170.

Sjöström, P. J., Turrigiano, G. G. and Nelson, S. B. (2001) 'Rate, timing, and cooperativity jointly determine cortical synaptic plasticity.', *Neuron*, 32(6), pp. 1149–1164. doi: 10.1016/s0896-6273(01)00542-6.

Song, S., Miller, K. D. and Abbott, L. F. (2000) 'Competitive Hebbian learning through spike-timing-dependent synaptic plasticity', *Nature Neuroscience*, 3(9), pp. 919–926. doi: 10.1038/78829.

Stoppini, L., Buchs, P. A. and Muller, D. (1991) 'A simple method for organotypic cultures of nervous tissue.', *Journal of Neuroscience Methods*, 37(2), pp. 173–82. doi: 10.1016/0165-0270(91)90128-M.

Suter, B. A. *et al.* (2010) 'Ephus: multipurpose data acquisition software for neuroscience experiments.', *Frontiers in Neural Circuits*, 4, p. 100. doi: 10.3389/fncir.2010.00100.

Testa-Silva, G. (2010) 'Human synapses show a wide temporal window for spike-timing-dependent plasticity', *Frontiers in Synaptic Neuroscience*. doi: 10.3389/fnsyn.2010.00012.

Tigaret, C. M. *et al.* (2016) 'Coordinated activation of distinct Ca2+ sources and metabotropic glutamate receptors encodes Hebbian synaptic plasticity', *Nature Communications*, 7, p. 10289. doi: 10.1038/ncomms10289.

Turrigiano, G. G. (2017) 'The dialectic of Hebb and homeostasis', *Philosophical Transactions of the Royal Society B: Biological Sciences*, 372(1715), p. 20160258. doi: 10.1098/rstb.2016.0258.

Wiegert, J Simon, Gee, C. E. and Oertner, T. G. (2017) 'Single-Cell Electroporation of Neurons.', *Cold Spring Harbor protocols*, 2017(2), pp. 135–138. doi: 10.1101/pdb.prot094904.

Wiegert, J. Simon, Gee, C. E. and Oertner, T. G. (2017) 'Viral Vector-Based Transduction of Slice Cultures.', *Cold Spring Harbor protocols*, 2017(2), pp. 131–134. doi: 10.1101/pdb.prot094896.

Wittenberg, G. M. and Wang, S. S. (2006) 'Malleability of spike-timing-dependent plasticity at the CA3-CA1 synapse', *Journal of Neuroscience*, 26(24), pp. 6610–6617. doi: 10.1523/JNEUROSCI.5388-05.2006.

Zhang, J.-C., Lau, P.-M. and Bi, G.-Q. (2009) 'Gain in sensitivity and loss in temporal contrast of STDP by dopaminergic modulation at hippocampal synapses.', *Proceedings of the National Academy of Sciences of the United States of America*, 106(31), pp. 13028–13033. doi: 10.1073/pnas.0900546106.

Figures and Tables

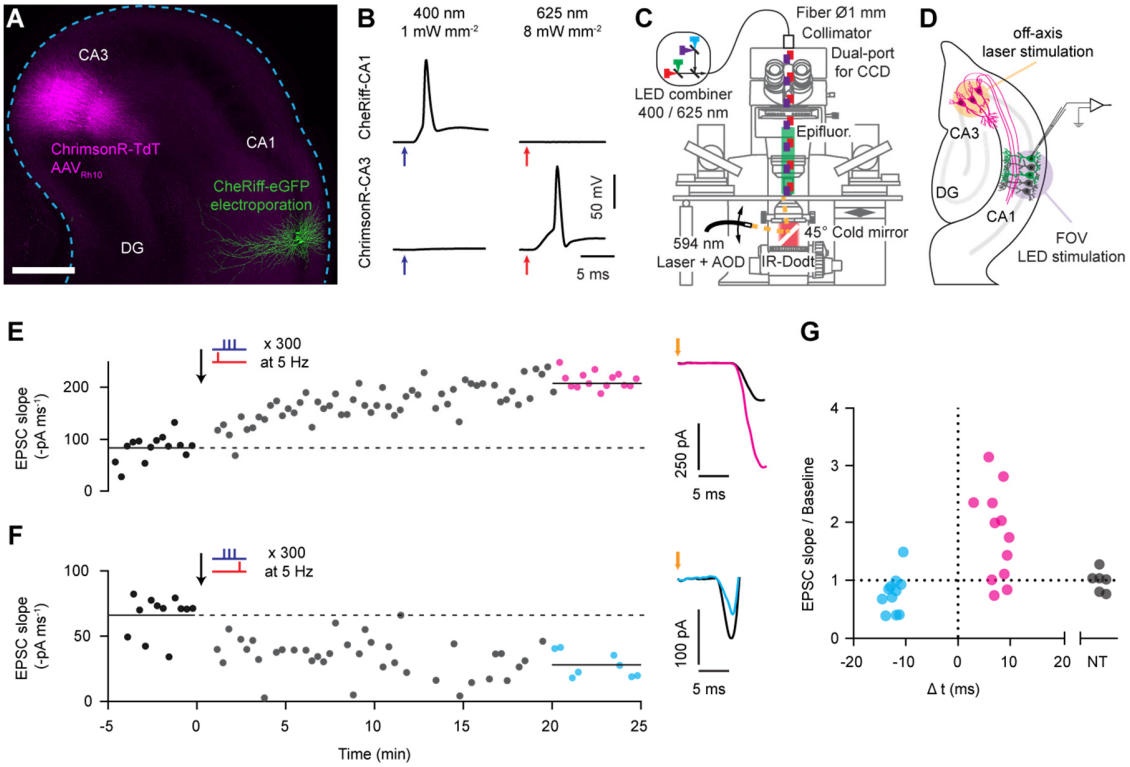

Figure 1. Optogenetic induction of spike-timing-dependent plasticity (oSTDP). A, Organotypic hippocampal slice culture, with ~30 CA3 neurons expressing ChrimsonR (magenta) and 3 CA1 neurons expressing CheRiff (green). Scale bar 500 µm. **B,** Example membrane responses of CheRiff-CA1 (upper traces) and ChrimsonR-CA3 (lower traces) neurons to 405 nm (violet arrows) and 625 nm (red arrows) light flashes (2 ms). Note that the CheRiff-CA1 neuron spikes and the ChrimsonR-CA3 neuron only slightly depolarizes in response to 405 nm light whereas in response to 625 nm light the ChrimsonR-CA3 neuron spikes and there is no response in the CheRiff-CA1 neuron. **C,** Diagram of the electrophysiological recording setup with on-axis LED and off-axis laser stimulation. **D,** Diagram of an organotypic hippocampal slice in the recording chamber. **E,** The slope of excitatory postsynaptic currents (EPSCs) recorded from one CheRiff-CA1 neuron in response to laser stimulation of ChrimsonR-CA3 neurons at baseline (black points) and after (grey and magenta points) causal pairing (t = 0, black arrow, one red (625 nm) and 12 ms later three violet (400 nm, 50 Hz) light flashes repeated 300 times at 5 Hz). At right are the averaged EPSCs from the black and magenta points, orange arrow shows time of laser flash to stimulate ChrimsonR-CA3 neurons. The magenta points were significantly potentiated relative to the baseline (black points), $p < 0.0001$, Kolmogorov-Smirnov. **F,** As in **E** but after anti-casual stimulation (three 400 nm light flashes preceded the 625 nm light flash by 8 ms). The cyan points were significantly depressed relative to baseline (black points), $p = 0.003$, Kolmogorov-Smirnov **G,** Average EPSC slope 20-25 minutes after oSTDP induction normalized to baseline from experiments as in **E** (magenta, n = 12) and **F** (cyan, n = 11), Δt is the actual EPSP-spike timing interval observed during the pairing (c.f. *SI Appendix Fig. S2*). NT, non-transfected neurons from slices subjected to causal pairing stimulation (n = 6). Magenta vs cyan points $p = 0.003$, Kolmogorov-Smirnov.

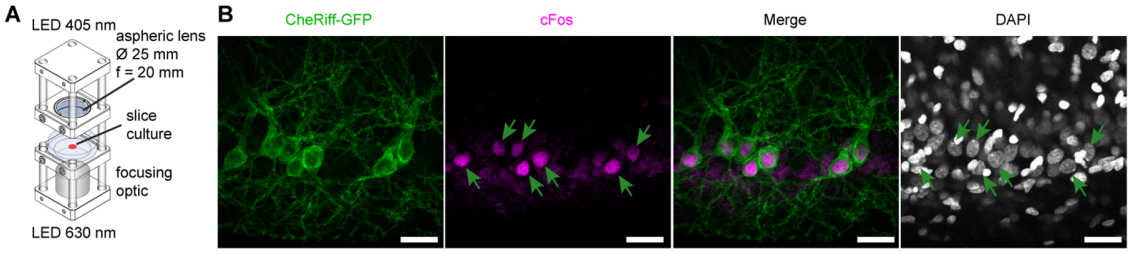

Figure 2. Activity-dependent cFos expression in CheRiff-CA1 neurons following in-incubator no-patch oSTDP. A, Diagram of the device used for in-incubator optogenetic stimulation of ChrimsonR-CA3 and CheRiff-CA1 neurons in hippocampal slice cultures. **B,** Expression of cFos in the CA1 region of a slice culture fixed 1.5 hours after causal in-incubator oSTDP stimulation. Confocal image stacks of CheRiff-CA1 neurons (green), anti-cFos (magenta) and overlay. At right are the DAPI stained nuclei. Green arrows point to nuclei of the CheRiff-CA1 neurons. Scale bars 50 µm.

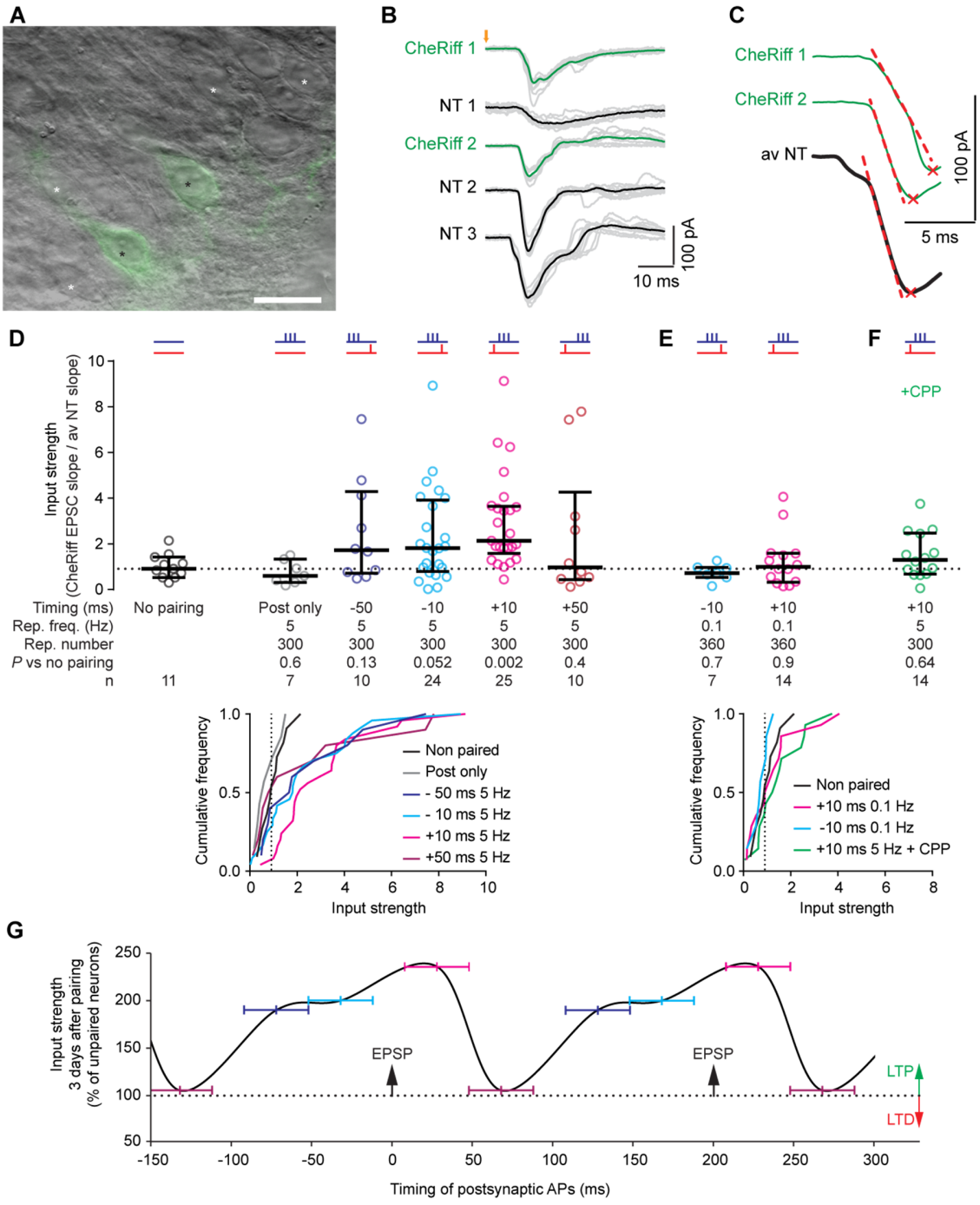

Figure 3 Three days after oSTDP only potentiation is evident. A, Dodt-contrast image (40x objective) of CA1 region with overlaid epifluorescence image. Black asterisks: CheRiff expressing CA1 pyramidal neurons; white asterisks: non-transfected CA1 pyramidal neurons suitable for recording. Note that the actual field of view is about 30% larger. Scale bar 25 µm. **B,** Laser stimulation (orange arrow, 1 ms, 594 nm) of ChrimsonR-CA3 neurons evoked excitatory postsynaptic currents (EPSCs) in CA1 neurons of a control (no oSTDP pairing) slice. EPSCs recorded sequentially from CheRiff-CA1 pyramidal neurons (green, average of 10 grey individual

EPSCs) and at least three non-transfected (NT) CA1 neurons (black average of 10 grey individual EPSCs). **C,** Automatically-detected EPSC peak (red x) and slope (dashed red line, 20-60% peak). EPSCs from NT neurons were averaged before determining the NT slope. **D,** Normalized input strength of CheRiff-CA1 neurons recorded from control (no pairing) slices and slices 3 days after pairing. At top red and violet ticks indicate order of pre- and postsynaptic stimulation, respectively. Plotted are individual data points, median and 25-75% interquartile range and cumulative frequency distributions (below). The dotted line is the median input strength onto CheRiff-CA1 neurons of the non-paired slices (median = 0.91). 'Timing' is the target interval between start of the EPSC and the first or last postsynaptic spike. 'Rep. freq.' is the pairing repetition frequency. 'Rep. num.' is the number of pairings. *P* values (Kolmogorov-Smirnov) are vs no pairing, n number of CheRiff-CA1 neurons in each experiment. **E,** As in **D** except the repetition frequency was reduced to 0.1 Hz for one hour. In all cumulative frequency plots the non-paired group was added as reference. **F,** As in **D** but the NMDA antagonist CPPene was in the culture medium during pairing (+CPP, 1 μM). **G,** Median input strength (% no pairing median) plotted relative to the light-induced EPSPs (arrows) and action potential timings (vertical ticks on colored bars) during oSTDP pairing (data from **E,** brown +50 ms, violet -50 ms, cyan -10 ms, magenta +10 ms). Two cycles (of 300) at 5 Hz are illustrated.

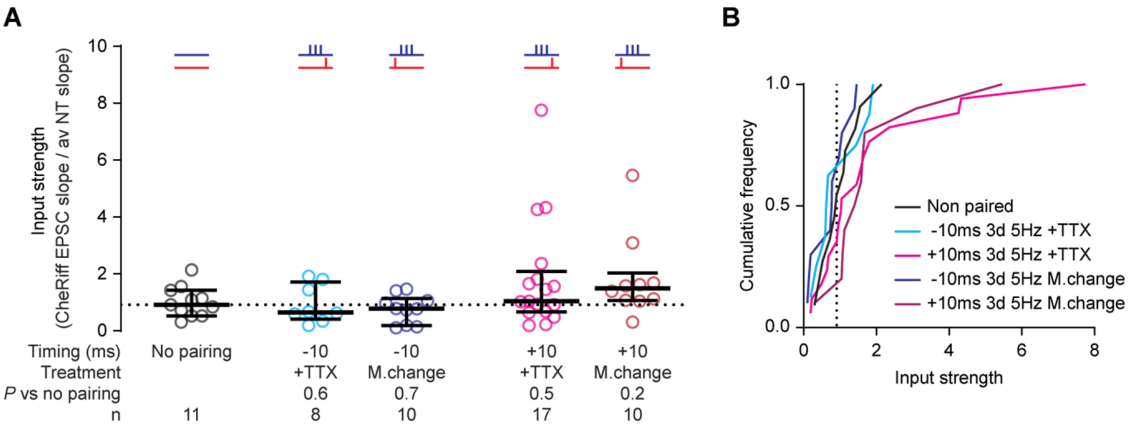

Figure 4. Activity in the paired pathway is essential for long term potentiation. A, Normalized input strength of CheRiff-CA1 neurons recorded from causally or anti-causally (300 rep at 5 Hz) paired slices 3 days later. The no pairing group is reproduced from Fig 3D. Three to four hours after oSTDP medium was changed (M. change) to increase global activity or activity was blocked with tetrodotoxin (+TTX, 1 µM). Two days later medium was changed again and TTX washed off. Plotted are individual data points, median and 25-75% interquartile range. P values (Kolmogorov-Smirnov) are vs no pairing group. **B,** Cumulative frequency distributions of **A**.

SI Appendix

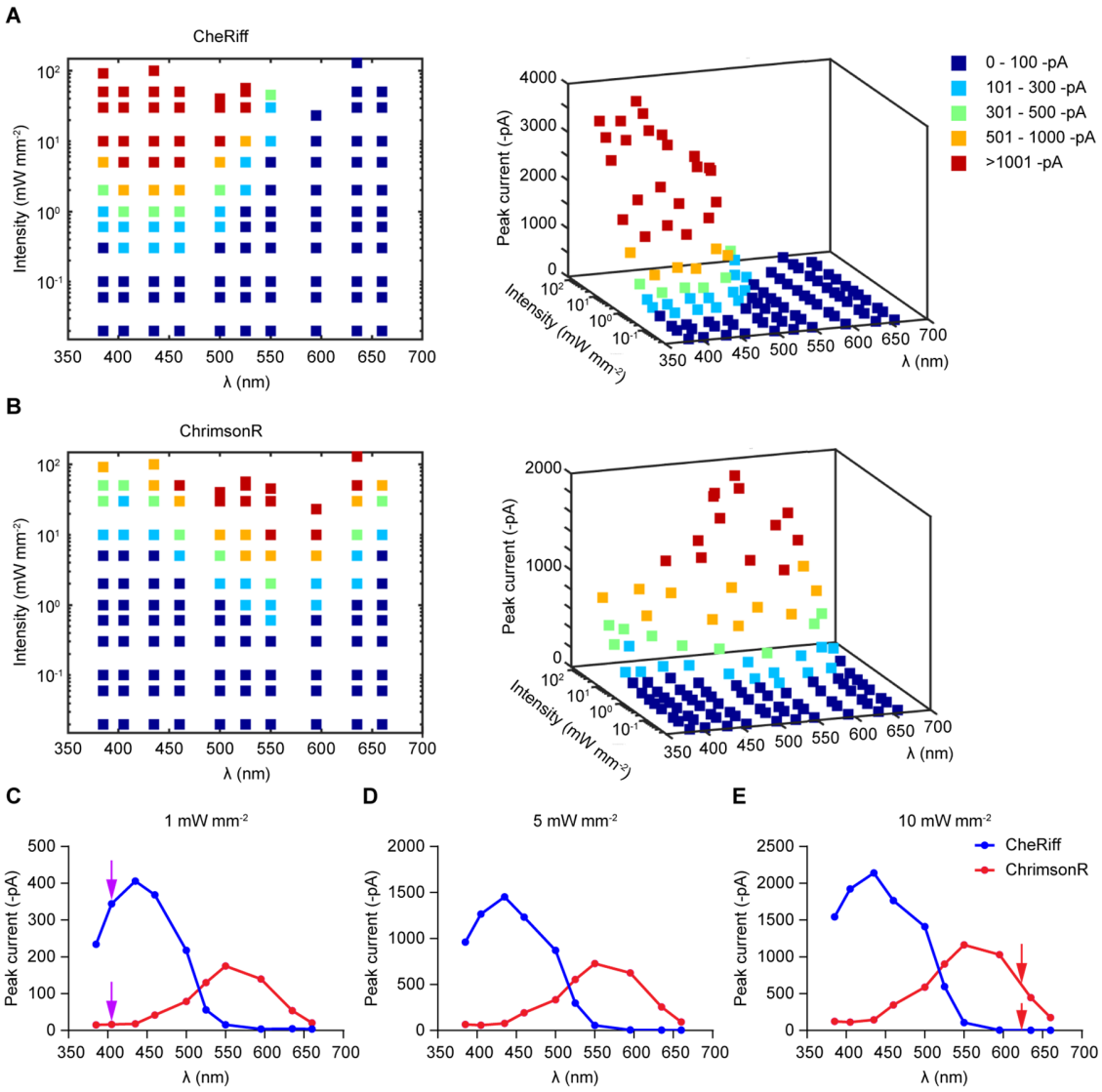

Supplementary Figure S1. CheRiff and ChrimsonR functional characterization. A, B, Average (n = 4 cells per point) light evoked EPSC peaks from CheRiff-CA1 neurons (electroporated) and ChrimsonR-CA3 neurons (AAV transduced) in response to stimulation with different wavelengths at different intensities. Color code indicates average peak current amplitude. Note that CheRiff-CA1 neurons were completely non-responsive to light with wavelengths longer than 550 nm and ChrimsonR-CA3 neurons were only modestly responsive to 405 nm light. Peak current vs wavelength at: **C,** 1 mW mm^{-2}, **D,** 5 mW mm^{-2} and **E,** 10 mW mm^{-2} for CheRiff-CA1 and ChrimsonR-CA3 neurons. Note different y-axis scales. Arrows indicate wavelengths/intensities used for oSTDP induction.

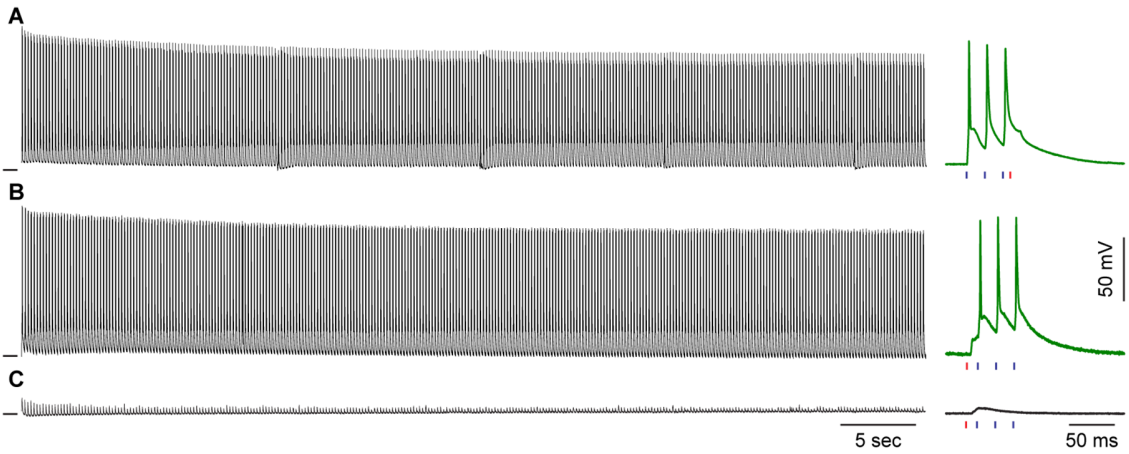

Supplementary Figure S2. Sample membrane responses of CA1 neurons during causal and anti-causal optical spike-timing-dependent plasticity pairing. A, Full recording (left) and time-expanded response (right) of a CheRiff-CA1 neuron during anti-causal pairing (-10 ms: 3 violet flashes at 50 Hz and 1 red flash 8 ms after, repeated 300x at 5 Hz). Note the EPSP following three spikes (right). Black ticks at far left indicate -70 mV. **B,** as in **A**, CheRiff-CA1 neuron during causal pairing (+10 ms: 1 red flash and 3 violet flashes at 50 Hz 12 ms after). Note the EPSP precedes the three spikes (right). **C,** Membrane voltage response of a non-transfected CA1 neuron during causal pairing. Note the EPSPs and absence of spikes.

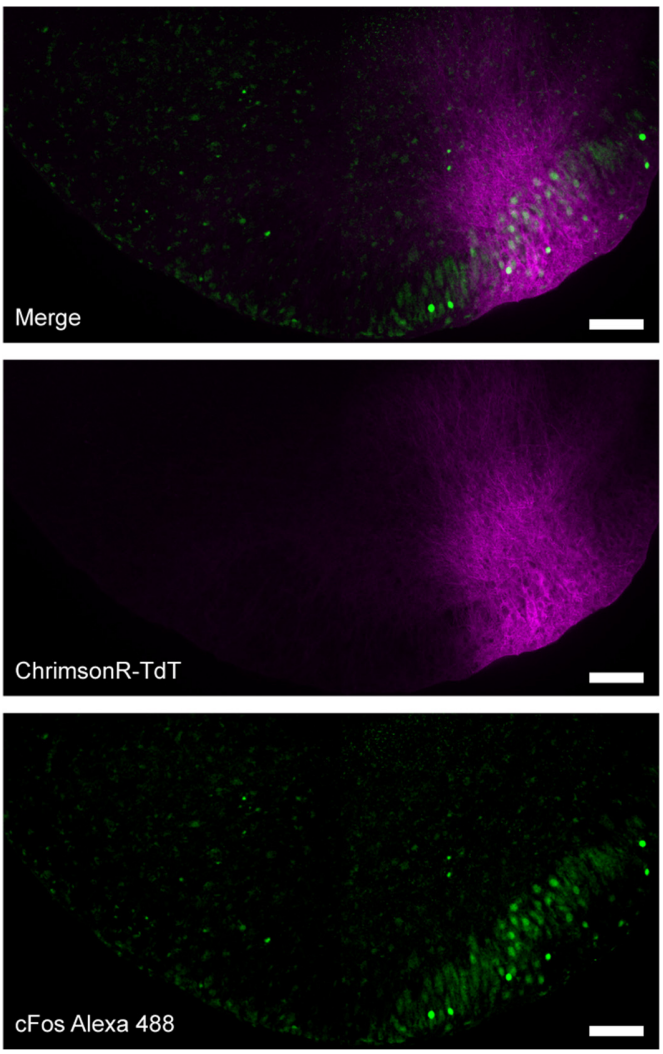

Supplementary Figure S3. CA3 neurons express cFos after burst firing. Confocal images of CA3 area of a hippocampal slice culture fixed 1.5 hours after burst stimulation (Blocked synaptic transmission: 1 µM CPPene, 100 µM Picrotoxin, 10 µM NBQX; red light: 3 flashes at 50 Hz repeated 300x at 5 Hz, 630 nm, 8 mW mm^{-2}). The ChrimsonR-tdTomato channel (magenta) is a minimum-intensity projection to visualize transfected neurons and a median-intensity projection was used for anti-cFos immunostaining (green). Approximately half of the burst-stimulated ChrimsonR-CA3 neurons were cFos-positive as were several non-transduced spontaneously active CA3 neurons. Scale bars 100 µm.

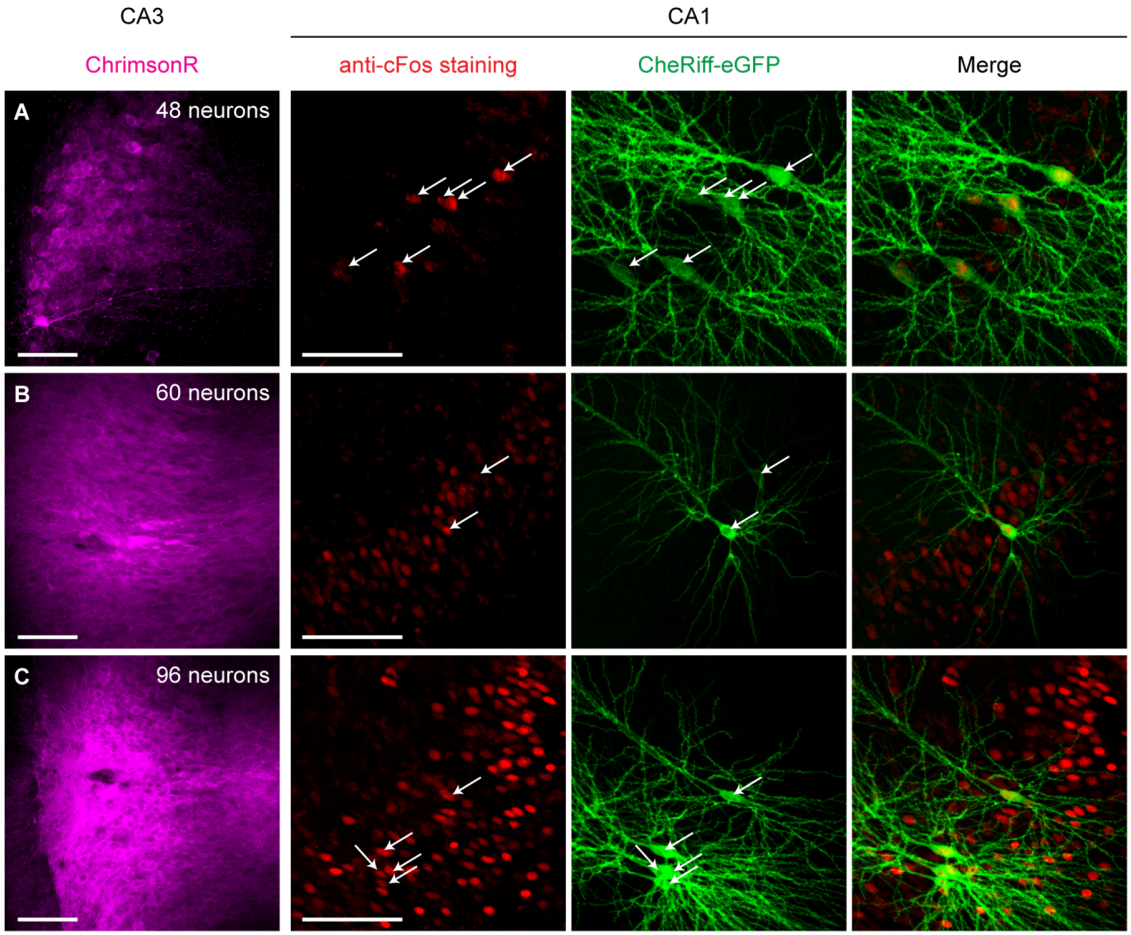

Supplementary Figure S4. cFos expression pattern after causal pairing vs number of ChrimsonR-CA3 neurons. Confocal images (average intensity projection) of CA3 and CA1 areas in a given slice culture. White arrows are showing the soma of CheRiff-CA1 neurons. Scale bars 100 µm. **A,** Expected cFos expression pattern in CA1 after causal pairing: Only directly light stimulated CheRiff-CA1 express cFos (5 out of 6). **B and C,** Number of ChrimsonR-CA3 neurons enough to induce complex spiking in CA1, which lead to cFos expression in NT-CA1 neurons.

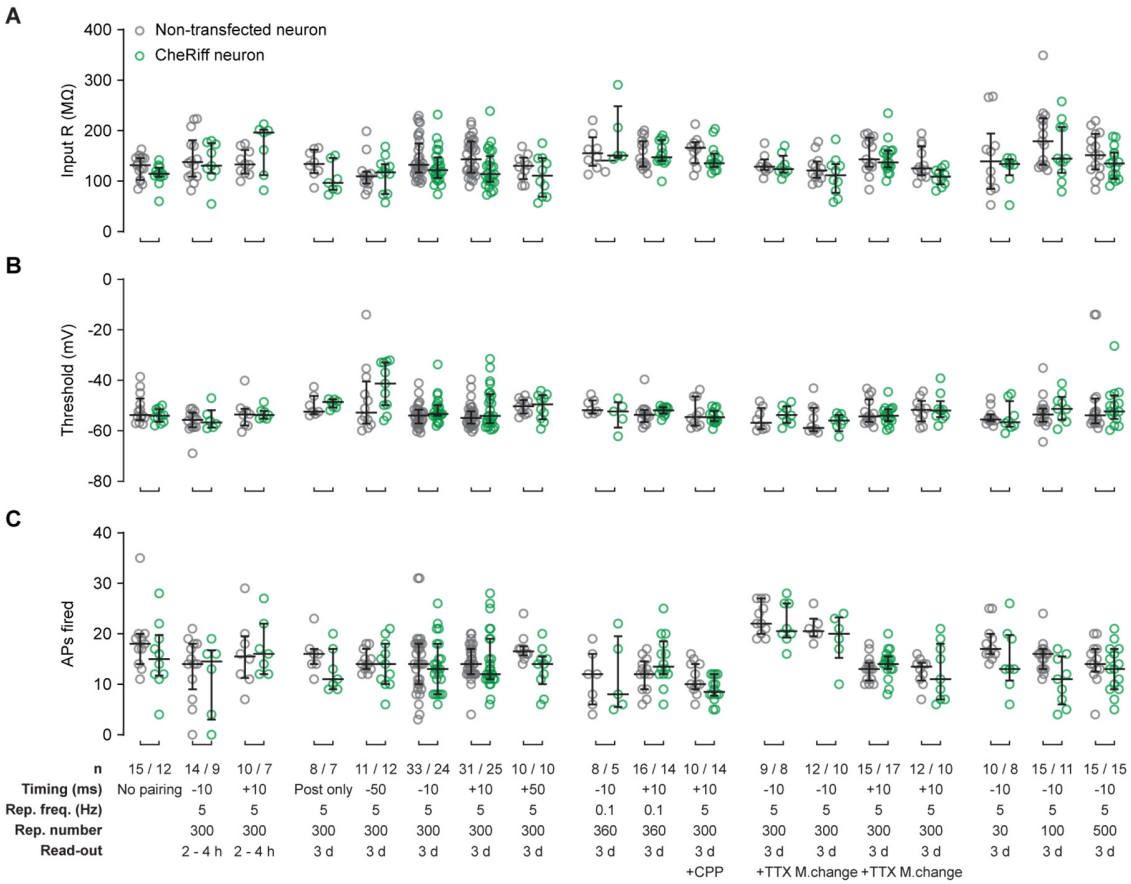

Supplementary Figure S5. Comparison of passive and active cell parameters of CheRiff-CA1 and neighboring NT-CA1 neurons from experiments in Fig. 3 and Fig. 4. A, Input resistance of all CheRiff-CA1 and NT neurons. **B,** Action potential threshold. **C,** Numbers of action potentials fired in response to a 400 pA current step. There were no significant differences between NT and CheRiff-CA1 neurons in any of the treatment groups (Kolmogorov-Smirnov). +CPP, 1 µM CPPene during oSTDP; +TTX, 1 µM tetrodotoxin 4-48 h after oSTDP; M. change, medium changed 4 and 48 h after oSTDP. *n* given as number of NT-CA1 / CheRiff-CA1 neurons.

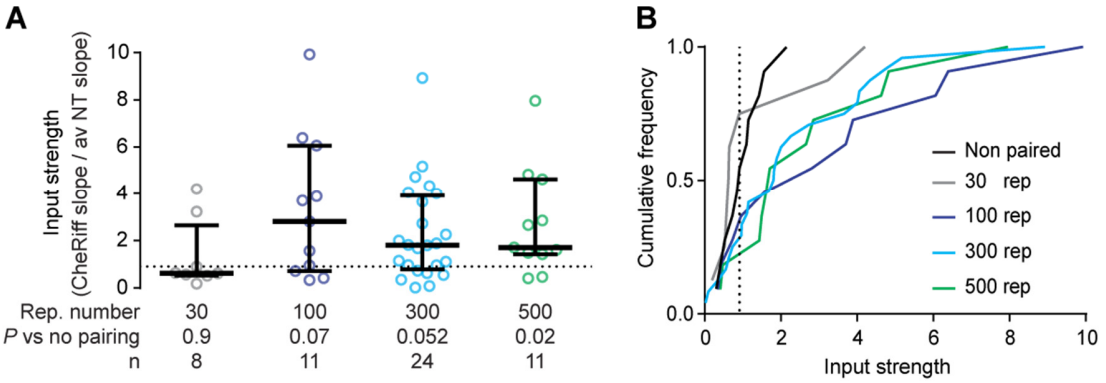

Supplementary Figure S6. Anti-causal pairing with different number of repeats still results in potentiation. A, Anti-causal pairing was applied as in Fig. 3 but the number of pairings at 5 Hz was varied as indicated (Rep. number). **B,** Cumulative frequency distributions. The non-paired and 300 repetition groups are duplicated from Fig. 3 for comparison. *P* values (Kolmogorov-Smirnov) are vs non-paired group from Fig.3.

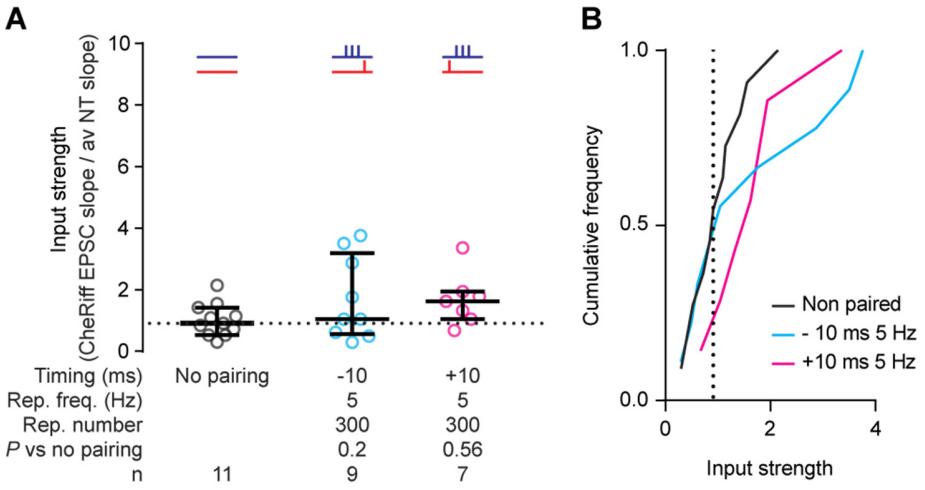

Supplementary Figure S7. Input strength is not changed 3 hours after oSTDP induction. A, Normalized input strength of CheRiff-CA1 neurons recorded from causally or anti-causally (300 rep at 5 Hz) paired slices approximately 3 hours later. The no pairing group is reproduced from Fig 3D. **B,** Cumulative frequency distributions. *P* values (Kolmogorov-Smirnov) are vs non-paired group.